The interference effect of laser-assisted bremsstrahlung emission in Coulomb fields of two nuclei

Ankang Li, Jiaxiang Wang, Na Ren, Pingxiao Wang, Wenjun Zhu, Xiaoya Li, Ross Hoehn, and Sabre Kais

Citation: Journal of Applied Physics **114**, 124904 (2013); doi: 10.1063/1.4822317
View online: http://dx.doi.org/10.1063/1.4822317
View Table of Contents: http://scitation.aip.org/content/aip/journal/jap/114/12?ver=pdfcov
Published by the AIP Publishing

The interference effect of laser-assisted bremsstrahlung emission in Coulomb fields of two nuclei

Ankang Li,[1] Jiaxiang Wang,[1,a)] Na Ren,[1] Pingxiao Wang,[2] Wenjun Zhu,[3] Xiaoya Li,[3] Ross Hoehn,[4] and Sabre Kais[4,5]
[1]*State Key Laboratory of Precision Spectroscopy and Department of Physics, East China Normal University, Shanghai 200062, China*
[2]*Applied Ion Beam Physics Laboratory, Key Laboratory of the Ministry of Education, China and Institute of Modern Physics, Department of Nuclear Science and Technology, Fudan University, Shanghai 200433, China*
[3]*National Key Laboratory of Shock Wave and Detonation Physics, Mianyang 621900, Sichuan, China*
[4]*Departments of Chemistry and Physics, Purdue University, West Lafayette, Indiana 47907, USA*
[5]*Qatar Environment and Energy Research Institute, Qatar Foundation, Doha, Qatar*

(Received 3 August 2013; accepted 11 September 2013; published online 27 September 2013)

In this paper, the spontaneous bremsstrahlung emission from an electron scattered by two fixed nuclei in an intense laser field is investigated in detail based upon the Volkov state and the Dirac-Volkov propagator. It has been found that the fundamental harmonic spectrum from the electron radiation exhibits distinctive fringes, which is dependent not only upon the internucleus distance and orientation but also upon the initial energy of the electron and the laser intensity. By analyzing the differential cross section, we are able to explain these effects in terms of interference among the electron scattering by the nuclei. These results could have promising applications in probing the atomic or molecular dressed potentials in intense laser fields. © *2013 AIP Publishing LLC*. [http://dx.doi.org/10.1063/1.4822317]

I. INTRODUCTION

High-order harmonic generation (HHG)[1–4] is a process in which high-order harmonics of the fundamental laser frequency are coherently radiated when an intense laser pulse is focused into an atomic or molecular gas. This process is not only used to generate UV or XUV lights but also be applied to explore molecular structures, recently. The first breakthrough was the discovery of a double-slit-type interference effect from the simplest diatomic molecules H_2^+ and H_2.[5–8] The experimental confirmation was first realized for aligned CO_2 in 2005.[9,10] The next major development was the so-called molecular orbital tomography proposed by Itatani *et al*. in 2004.[11] Namely, once the HHG spectra and phases are known for various orientation of molecular axis, a 2D projection of the initial electron orbital can be reconstructed through a tomographic algorithm. Now, the work has been generalized to include orbital symmetry influences upon HHG and quantum tomography with 2D calculations.[12]

In all the above-mentioned works, the HHG originates from the electrons bound by the atoms or molecules and the calculation usually involves the time-dependent Schrodinger equation (TDSE) with dipole approximation. But when the field is so strong that the ponderomotive energy of the free electron reaches the same order of the rest energy of the electron, there will be a different picture. Namely, the dipole approximation may not be a good choice and the TDSE should be replaced by the Dirac equation. Moreover, some electrons may be ionized to be free particles, whose dynamics will be predominated by the intense laser fields instead of the Coulomb potentials. Now, the principle process is the so-called laser-assisted bremsstrahlung, which has been studied previously by several authors. In the early works, the analytic expression for the radiation spectrum of laser-assisted bremsstrahlung in a plane monochromatic has been derived by Karapetyan and Fedorov for nonrelativistic regime.[13] Within the framework of the Born approximation, Roshchupkin[14,15] has developed a general relativistic expression for the amplitude of the scattering of an electron by a nucleus in an external field with arbitrary intensity. Recently, the numerical evaluation of the laser-assisted bremsstrahlung process has been carried out for both circularly polarized and linearly polarized laser field.[16,17]

Motivated by the molecule HHG in non-relativistic case, in this paper, we will consider an electron scattering by two nuclei in strong laser fields. This model differs from one-nucleus case mentioned above by providing more than one center for the electron scattering, which will allow for dynamics, for example, the emission spectra of the electron may depend on the internuclear distance and orientation, just as in the situation of molecule HHG. This model could provide us a method to explore some special potentials, which exists only in intense laser fields, such as the dressed Kramer-Henneberg potential in high-frequency laser fields, which plays an important role in guaranteeing the existence of multiply charged negative ions in the fields.

The notations used in this paper are as follows. The four-vector product is denoted by $a \cdot b = a^0 b^0 - \boldsymbol{ab}$. For the Feynman dagger, we use the following notation: $\not{A} = \gamma \cdot A$. The Dirac adjoint is denoted by the standard notation $\bar{u} = u^\dagger \gamma^0$ for a bispinor u and $\bar{F} = \gamma^0 F^\dagger \gamma^0$ for a matrix F.

The outline of this paper is as follows. First, we will introduce the laser-assisted bremsstrahlung model and derive

a)Author to whom correspondence should be addressed. Electronic mail: jxwang@phy.ecnu.edu.cn

the theoretical expression for the cross section of the emission in Sec. II. Then, the numerical estimation of the cross section and the corresponding analyses will be provided in Sec. III. Concluding remarks are reserved for Sec. IV.

II. THEORETICAL DERIVATION OF THE BREMSSTRAHLUNG CROSS SECTION

Consider two nuclei with charge number Z fixed in the x-z plane with an internucleus distance R_0 in a strong laser field. We assume that, in the laboratory frame of reference, the laser can be described by a plane wave propagating in the positive direction of the z-axis with a vector potential A^μ

$$A^\mu = A_0[\delta \cos\phi \epsilon_1{}^\mu + (1-\delta^2)^{1/2}\sin\phi\epsilon_2{}^\mu]. \tag{1}$$

The approximation is acceptable if the number of laser photons is large enough so that an arbitrary amount of energy and momentum can be taken from or emitted into the field without changing it. The plane wave depends only on the phase factor $\phi = k\cdot x$, in which x is the position vector, and $k^\mu = \frac{\omega_0}{c}(1,0,0,1)$ the four wave vector with ω_0 denoting the laser frequency. The laser is circularly polarized for $\delta = 1/\sqrt{2}$ and linearly polarized for $\delta = 0, \pm 1$. We define two polarization vectors ϵ_1, ϵ_2, satisfying $\epsilon_i \cdot k = 0$, $\epsilon_i \cdot \epsilon_j = \delta_{ij}$ $(i, j = 1, 2)$. The laser intensity can be easily described by a dimensionless parameter $Q = eA_0/(mc^2)$, which is usually called laser intensity parameter. It should be mentioned that in the nonrelativistic regime, the characteristic velocity and energy for an electron moving in such an electromagnetic field is $v \sim eA_0/(mc)$ and $E \sim e^2A_0^2/(mc^2)$, so a relativistic treatment is necessary if $v \sim c$ and $E \sim mc^2$ is satisfied, which means the motion of the electron will become relativistic when $Q \sim 1$.

The angle between the orientation of two nuclei and the laser propagation direction is denoted by ϑ. For convenience of calculation, here we set the origin of the coordinate at the middle of two nuclei. So we can easily introduce a vector $\boldsymbol{R} = R_0(\sin\vartheta \boldsymbol{e_x} + \cos\vartheta \boldsymbol{e_z})/2$ to describe the location of the two nuclei.

Now we begin to derive the differential cross section of the electron-nucleus bremsstrahlung. Consider the scattering geometry that an incoming electron moving along the negative z-axis has a head-on collision of the laser photons while scattering by two nuclei. The configuration is shown in Fig. 1. The whole process can be described by two Feynman diagrams displayed in Fig. 2. In the first one, the initial electron first interacts with two nuclei and then emits a bremsstrahlung photon. The situation is reversed in the second diagram. In Feynman diagrams, the electron is denoted by a zigzag line on top of a straight line since it is dressed by a strong laser. Also, here the free electron propagator is replaced by the Dirac-Volkov propagator.[18]

Actually, the electron will interact with three external fields during the process, namely, the laser field described by Eq. (1), the Coulomb field of two nuclei, and the field of the emitted bremsstrahlung photon. As usual, we treat the laser-electron interaction exactly and nonperturbatively by using Volkov states as the initial and final wave functions

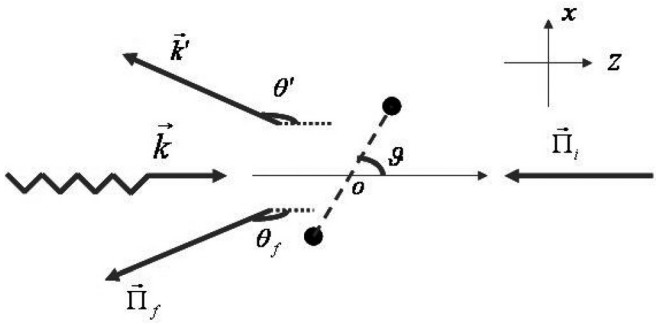

FIG. 1. The scattering geometry: The incoming electron with laser-dressed four momentum Π_i counterpropagates with the laser, while scattering by two fixed nuclei. ϑ is an angle between internucleus axis and the laser propagating direction. The final electron with Π_f and the bremsstrahlung photon with k' are projected onto the xz plane in this figure; so, only the polar angles θ_f and θ' are displayed. The azimuthal angles are denoted by Ω_f and Ω', respectively.

$$\psi_{p,r} = \sqrt{\frac{mc}{\Pi^0 V}}\zeta_p(x)u_r(p), \tag{2}$$

$$\zeta_p(x) = \left(1 + \frac{e\not{k}\not{A}}{2p\cdot k}\right)e^{iS}, \tag{3}$$

$$S = -\frac{\Pi\cdot x}{\hbar} - \frac{e^2A_0^2}{8\hbar c^2(p\cdot k)}(2\delta^2-1)\sin 2\phi + \frac{eA_0}{\hbar c(p\cdot k)} \times [\delta(p\cdot\epsilon_1)\sin\phi - (1-\delta^2)^{1/2}(p\cdot\epsilon_2)\cos\phi]. \tag{4}$$

Here, p is the four-momentum of the electron outside the field, and $\Pi = p + \frac{e^2A_0^2}{4c^2(p\cdot k)}$ is the corresponding laser-dressed four-momentum, $u_r(p)$ the free Dirac spinor. Here, we employ a box normalization with a normalized volume V.

The interaction with the emitted radiation and Coulomb field is taken to the first perturbation, in which the interaction between electron and nuclei is considered under Born approximation: $v_i/c \ll \alpha Z$. Here, α is fine structure constant and v_i is the initial velocity of the electron. As to the Coulomb field of the nuclei, we use a Yukawa potential with a screen length l_0 instead of the conventional Coulomb potential to avoid possible singularity at resonance. The four-vector potential of the two fixed nuclei can be written as

$$A_Y^\mu(\boldsymbol{r}) = -\frac{Ze\delta^{\mu 0}}{|\boldsymbol{r}-\boldsymbol{R}|}e^{|\boldsymbol{r}-\boldsymbol{R}|/l_0} - \frac{Ze\delta^{\mu 0}}{|\boldsymbol{r}+\boldsymbol{R}|}e^{|\boldsymbol{r}+\boldsymbol{R}|/l_0}. \tag{5}$$

The corresponding Fourier transform is

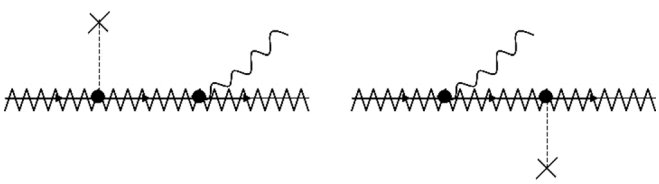

FIG. 2. Feynman diagrams describing laser-assisted bremsstrahlung. The laser-dressed electron and laser-dressed electron propagator are denoted by a zigzag line on top of the straight line. The Coulomb field photon is drawn as a dashed line, and the bremsstrahlung photon as a wavy line.

$$A_Y^{\mu}(\boldsymbol{q}) = -\frac{4\pi Ze}{\boldsymbol{q}^2 + l_0^2}(e^{i\boldsymbol{qR}} + e^{-i\boldsymbol{qR}}). \tag{6}$$

As we can see, the Fourier transform of the potential depends on the inter-distance and the orientation of the two nuclei. This is the origin of the interference effect on the radiation spectrum. The four-vector potential of the emitted bremsstrahlung photon has the form

$$A_c^{\mu}(x) = \sqrt{2\pi\hbar/\omega'}c\epsilon_c{}^{\mu}e^{ik'x}. \tag{7}$$

The wave vector of the emitted photon with polarization is described by $k' = \frac{\omega'}{c}(1, \boldsymbol{e_{k'}})$, $\boldsymbol{e_{k'}} = \cos\varphi'\sin\theta'\boldsymbol{e_x} + \sin\varphi'\sin\theta'\boldsymbol{e_y} + \cos\theta'\boldsymbol{e_z}$. So, the transition amplitude of an electron scattering by two fixed nuclei in a strong laser field can be specified by the following expression:

$$\begin{aligned} S_{fi} = -\frac{e^2}{\hbar^2c^2}\int dx^4dy^4\bar{\psi}_{p_f,r_f}(x)[\not{A}_c(x)iG(x-y)\not{A}_Y(y) \\ + \not{A}_Y(x)iG(x-y)\not{A}_c(y)]\psi_{p_i,r_i}(y). \end{aligned} \tag{8}$$

Here, $iG(x-y)$ is the laser-dressed propagator of the electron, which can be written as

$$iG(x-y) = -\int\frac{dp^4}{(2\pi\hbar)^3(2\pi i)}\zeta_p(x)\,\frac{\not{p}+mc}{p^2-m^2c^2}\,\bar{\zeta}_p(y). \tag{9}$$

Since we are not interested in investigating polarization or spin properties, we average over the spin of the incoming electron, and sum over the spin and polarization of the final electron. The differential cross section is calculated with the formula

$$d\tilde{\sigma} = \frac{1}{2JT}\sum_{r_i,r_f,\varepsilon_c}|S_{fi}|^2\frac{Vd^3\Pi_f}{(2\pi\hbar)^3}\frac{d^3k'}{(2\pi)^3}. \tag{10}$$

Here, T is the long observation time and $J = \frac{c}{V}\frac{\boldsymbol{\Pi_i}}{\Pi_i^0}$ stands for the incoming particle flux. We have $d^3\boldsymbol{\Pi_f} = |\boldsymbol{\Pi_f}|^2d\Omega_f = |\boldsymbol{\Pi_f}|^2\sin\theta_f d\theta_f d\varphi_f$, $d^3k' = \frac{\omega'^2}{c^2}d\Omega' = \frac{\omega'^2}{c^2}\sin\theta' d\theta' d\varphi'$, where Ω' and Ω_f are solid angle for the emitted photon and electron, respectively. Finally, we can derive the expression of the average differential cross section for emission or absorption of n photons as (for details, see Appendix)

$$\begin{aligned} \frac{d\tilde{\sigma}}{d\omega' d\Omega' d\Omega_f} = \frac{\alpha(Z\alpha)^2}{8\pi^2c^2}\sum_{n,\varepsilon_c}\frac{|\boldsymbol{\Pi_f}|}{|\boldsymbol{\Pi_i}|}|e^{i\boldsymbol{qR}} + e^{-i\boldsymbol{qR}}|^2 \\ \times\frac{\omega'}{(\boldsymbol{q}^2+l_0^2)^2}Tr[\bar{R}_{fi,n}(p_f+mc)R_{fi,n}(p_i+mc)], \end{aligned} \tag{11}$$

where

$$\begin{aligned} R_{fi,n} = \sum_s M_{-n-s}(\not{\epsilon}_c, \eta^1_{\Pi,\Pi_f}, \eta^2_{\Pi,\Pi_f})\frac{i}{\not{p}-mc} \\ \times\bar{M}_{-s}(\gamma^0, \eta^1_{\Pi,\Pi_i}, \eta^2_{\Pi,\Pi_i}) \\ +\sum_{s'}M_{-n-s'}(\gamma^0, \eta^1_{\Pi',\Pi_f}, \eta^2_{\Pi',\Pi_f})\frac{i}{\not{p}'-mc} \\ \times\bar{M}_{-s'}(\not{\epsilon}_c, \eta^1_{\Pi',\Pi_i}, \eta^2_{\Pi',\Pi_i}), \end{aligned} \tag{12}$$

with the argument defined as

$$\begin{aligned} \eta^1_{p_1,p_2} &= \frac{eA_0}{\hbar c}\delta\left[\frac{p_2\cdot\epsilon_1}{k\cdot p_2} - \frac{p_1\cdot\epsilon_1}{k\cdot p_1}\right], \\ \eta^2_{p_1,p_2} &= -\frac{eA_0}{\hbar c}(1-\delta^2)^{1/2}\left[\frac{p_2\cdot\epsilon_1}{k\cdot p_2} - \frac{p_1\cdot\epsilon_1}{k\cdot p_1}\right]. \end{aligned} \tag{13}$$

The four-momentum transfer onto the Coulomb field by two fixed nuclei is denoted by $q^{\mu} = (0, \boldsymbol{q})$, and the two laser-dressed four-momenta of the virtual electrons in the Feynman diagrams by Π, Π'. They are given by the energy-momentum conserving relation during the scattering process

$$\begin{aligned} \Pi &= \pi_f - (n+s)\hbar k + \hbar k', \\ \Pi' &= \pi_i - s\hbar k - \hbar k', \\ \hbar q &= \pi_f - \pi_i + \hbar k' - n\hbar k. \end{aligned} \tag{14}$$

M is a 4×4 matrix with five arguments

$$\begin{aligned} M_s(F, \eta^1_{p_1,p_2}, \eta^2_{p_1,p_2}) \\ = \left[\not{F} + \frac{e^2A_0{}^2}{8c^2}\frac{\not{k}\not{F}\not{k}}{(p_i\cdot k)(p_2\cdot k)}\right]G_s^0(\alpha,\beta,\varphi) \\ + \frac{eA_0}{2c}\delta\left[\frac{\not{\epsilon}_1\not{k}\not{F}}{(p_1\cdot k)} + \frac{\not{F}\not{k}\not{\epsilon}_1}{(p_2\cdot k)}\right]G_s^1(\alpha,\beta,\varphi) \\ + \frac{eA_0}{2c}(1-\delta^2)^{1/2}\left[\frac{\not{\epsilon}_2\not{k}\not{F}}{(p_1\cdot k)} + \frac{\not{F}\not{k}\not{\epsilon}_2}{(p_2\cdot k)}\right]G_s^2(\alpha,\beta,\varphi) \\ + \left(\delta^2 - \frac{1}{2}\right)\frac{e^2A_0{}^2}{4c^2}\frac{\not{k}\not{F}\not{k}}{(p_i\cdot k)(p_2\cdot k)}G_s^3(\alpha,\beta,\varphi). \end{aligned} \tag{15}$$

The generalized Bessel functions are given by

$$\begin{aligned} G_s^0(\alpha,\beta,\varphi) &= \sum_n J_{2n-s}(\alpha)J_n(\beta)e^{i(s-2n)\varphi}, \\ G_s^1(\alpha,\beta,\varphi) &= \frac{1}{2}(G_{s+1}^0(\alpha,\beta,\varphi) + G_{s-1}^0(\alpha,\beta,\varphi)), \\ G_s^2(\alpha,\beta,\varphi) &= \frac{1}{2i}(G_{s+1}^0(\alpha,\beta,\varphi) - G_{s-1}^0(\alpha,\beta,\varphi)), \\ G_s^3(\alpha,\beta,\varphi) &= \frac{1}{2}(G_{s+2}^0(\alpha,\beta,\varphi) + G_{s-2}^0(\alpha,\beta,\varphi)). \end{aligned} \tag{16}$$

With the corresponding argument,

$$\begin{aligned} \alpha &= \left[(\eta^1_{p_1,p_2})^2 + (\eta^2_{p_1,p_2})^2\right]^{1/2}, \\ \beta &= \frac{Qm^2c^2}{8\hbar}(2\delta-1)\left(\frac{1}{k\cdot p_1} - \frac{1}{k\cdot p_2}\right) \\ \varphi &= arctan\left(-\frac{\eta^2_{p_1,p_2}}{\eta^1_{p_1,p_2}}\right). \end{aligned} \tag{17}$$

The differential cross section in Eq. (11) is evaluated for both the direction of the final electron and the bremsstrahlung photon. Here, we are more interested in the influence by the internuclear distance and orientation on the bremsstrahlung photon spectrum, so we integrate the differential cross section over the solid angle Ω_f of the outgoing electron and obtain a cross section differential only in the direction of the emitted bremsstrahlung photon and its energy

$$\frac{d\sigma}{d\omega' d\Omega'} = \int \frac{d\tilde{\sigma}}{d\omega' d\Omega' d\Omega_f} d\Omega_f. \tag{18}$$

It is well known that the resonance occurs when the intermediate electron falls within the mass shell.[14–17] That is because the lower order processes (here refers to the nonlinear Compton scattering) are allowed in the field of a light wave. Although the resonance is a characteristic feature of the second-order process like bremsstrahlung, but it will not draw much of our attention here since the cross section (18) at resonance will not be affected by the internuclear distance or orientation, for which the screening length need not be discussed here. More details will be given in Sec. III.

III. NUMERICAL RESULTS

In this section, we will present some examples of the cross section in Eq. (18) for different internuclear distance or orientation. We consider the internuclear distance of two fixed proton ($Z = 1$) is about several atom units. To observe the effect of the Coulomb field of two fixed nuclei on the spectra, we have to choose the laser frequency in an X-rays order: the wavelength is 0.2 nm. The intensity of the laser is $Q = 17.8$ and circularly polarized. First, we consider the electron has an initial energy of $E_i = 5$ MeV and the orientation of the two nuclei is parallel to the direction of laser propagation. The cross section of the fundamental harmonic for scattering angle $\theta' = 1^\circ$ is shown in Fig. 3. The most remarkable feature of the spectrum is that there are minima at some frequencies for large internuclear distance.

The mechanism behind this phenomenon is two-centre interference during the scattering process, which is described by the term $\zeta(\boldsymbol{q},\boldsymbol{R}) = |e^{i\boldsymbol{q}\boldsymbol{R}} + e^{-i\boldsymbol{q}\boldsymbol{R}}|^2 \sim \cos^2(\boldsymbol{q}\cdot\boldsymbol{R})$ in the cross section. So when the momentum transfer from the Coulomb field is so large that $\boldsymbol{q}\cdot\boldsymbol{R} \sim 1$, the differential cross section in Eq. (11) will be suppressed for some special condition. Since most of the contribution to the integrand (18) comes from a small cone in the forward direction of the ingoing electron ($\theta_f = \pi$), the positions of the minima found in the spectra are largely determined by the parameter $\zeta(\boldsymbol{q},\boldsymbol{R})$ in the backscattering direction. This can be confirmed in Fig. 4, which plots $\zeta(\boldsymbol{q},\boldsymbol{R})$ as a function of harmonic frequency for emission angle $\theta_f = \pi$. The positions of the minima in the spectra are almost coincident with those of $\zeta(\boldsymbol{q},\boldsymbol{R})$, which can be expected for the condition

$$R_0 \cdot \cos\vartheta/2 = 2\pi(l + \frac{1}{2})/|\boldsymbol{q}|, \quad l = (1, 2, 3, ...). \tag{19}$$

That is interesting because we can deduce the internucleus distance by estimating the momentum transfer through the conservation relationship (14). It is obvious that $\zeta(\boldsymbol{q},\boldsymbol{R})$ is at its peak at the resonances regardless of the internuclear distance. This can be explained by considering that the momentum transfer onto the nucleus is almost zero when the resonance condition is satisfied (i.e., the intermediate electron becomes real). That is to say, the resonance peak of the spectrum carries little information about the internuclear distance or orientation, for which we will not pay much attention to the phenomenon of resonance.

The dependence of the differential cross section in Eq. (18) on the electron emission angle θ_f at frequency $\omega' = 0.955\omega_0$ is plotted in Fig. 5. It is located close to one of the minima in the spectrum. We observe a clear suppression of the emission at small angle around the direction of the ingoing electron for $R_0 = 1$ nm, which result in the minimum of the spectrum. As can be expected from Eq. (19), if we increase the angle between the orientation of the two nuclei and the direction of the laser propagation, the two-centre interference will be less effective. Finally, we even could not find a pronounced minimum in the spectrum when the internucleus orientation is perpendicular to the direction of the laser propagation ($\vartheta = \frac{\pi}{2}$). In order to corroborate this idea, we plot the full cross section for $\vartheta = \pi/2$ in comparison with that of $\vartheta = 0$ for the same internucleus distance in

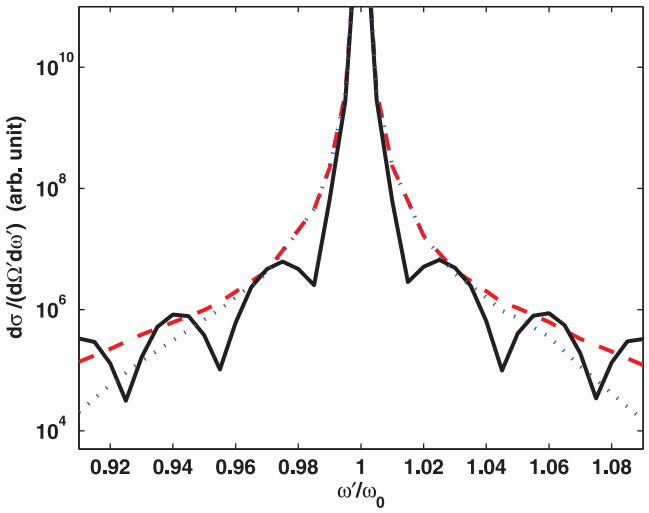

FIG. 3. The cross section for the fundamental harmonic at $\theta' = 1^\circ$. Here, we consider an electron with initial energy 5 MeV head-collide with a circularly polarized laser with intensity parameter $Q = 17.8$ and is scattered by two fixed nuclei. The internucleus distance is 1 nm for the full line, 0.152 nm for the dotted line, and 0.1 nm for the dashed line.

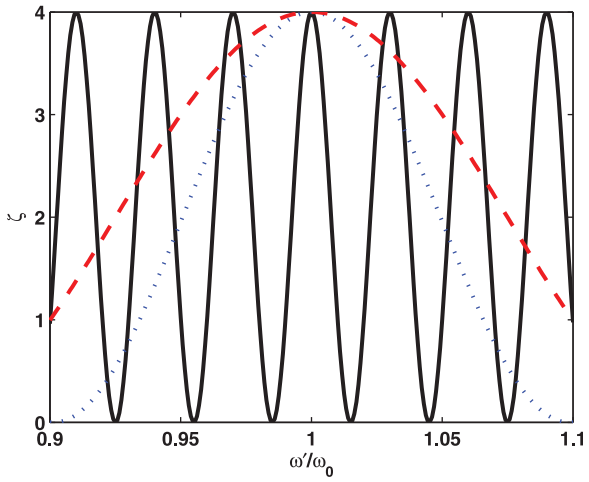

FIG. 4. The relation between the parameter $\zeta(\boldsymbol{q},\boldsymbol{R})$ and the bremsstrahlung photo frequency ω' at $\theta_f = \pi$ for absorbing 1 photon in the whole process (n = 1). The parameter of the electron and laser is the same with Fig. 3. The internucleus distance is 1 nm for the full line, 0.152 nm for the dotted line, and 0.1 nm for the dashed line.

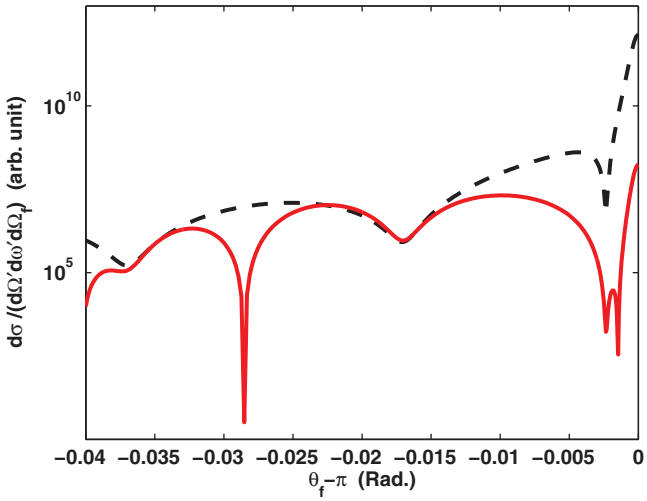

FIG. 5. The differential cross section as a function of the electron emission angle θ_f for the fundamental harmonic for absorbing 1 photon in the whole process (n = 1). The parameter of the electron and laser is the same with Fig. 3. The internucleus distance is 1 nm for the full line and 0.1 nm for the dashed line.

Fig. 6. The explanation for this phenomenon is that the momentum transfer from the Coulomb field q is mainly in the backscattering direction according to the conservation relationship (14), thus $\boldsymbol{q}\cdot\boldsymbol{R}\approx 0$. We can conclude that the more projection of the internucleus distance onto the laser propagating direction, the more oscillation occurs for the parameter $\zeta(\boldsymbol{q},\boldsymbol{R})$, which leads to the appearance of the minima in spectrum. The initial velocity of the ingoing electron also has a large effect on this two-centre interference phenomenon. That is because it will influence the momentum transfer from the Coulomb field to the electron. Here, we still set $(\vartheta = 0)$ to maximize the two-centre interference. To have a clear idea of the relation between the initial velocity v_i and the momentum transfer from the Coulomb field on the internucleus orientation q^4, we shall calculate the derivative dq^4/dv_i for fundamental harmonics. From the conservation relationship, we have (here we set $\hbar = m = c = 1$)

$$\frac{dq^4}{dv_i} = \left[\frac{1-\dfrac{1+Q^2/2}{(\pi_i^0)^2}}{1-\dfrac{1+Q^2/2}{(\pi_i^0+\Delta\omega)^2}}\right]^{1/2}\cos(\theta_f-\pi)-1. \tag{20}$$

Here, $\Delta\omega = \omega' - \omega_0$. For $\theta_f \approx \pi$, we could learn there will be more momentum transfer for smaller initial velocity based on Eq. (19). Remembering the interference is in connection with the term $\zeta(\boldsymbol{q},\boldsymbol{R}) \sim \cos^2(\boldsymbol{q}\cdot\boldsymbol{R})$, so we expect there will be more minima on the spectrum for "slow" electron but still satisfying the Born approximation, as can be seen from Fig. 7. Here, we compare the spectrum for initial electron energy $E_i = 3.5$ MeV with that of $E_i = 5$ MeV. The locations of the minima on the spectrum are different and the interval is smaller for $E_i = 3.5$ MeV, which confirms our opinion. For the same reason, we expect this will also happen with the increasing laser intensity since the electron is more decelerated by the light pressure of a counterpropagating laser.

It has to be mentioned that the parameter ($Q = 17.8$ with a wavelength of 0.2 nm) we choose in the paper will correspond to an X-ray laser with intensity up to $I = 10^{28}$ W/cm^2, which, according to an optimistic view,[19] could be reached with future upgrades of the FLASH facility in Hamburg. On the other hand, considering a neodymium laser with a frequency of 1.17 eV and $Q = 17.8$ (corresponding to an intensity $I = 10^{28}$W/cm^2), the clear interference effect of laser-assisted bremsstrahlung emission also could be found when $\boldsymbol{q}\cdot\boldsymbol{R}\sim 1$ is satisfied. That is to say, the corresponding internucleus distance has to be on an order of micrometer ($\boldsymbol{R}\sim 10^{-6}$m) according to our calculation. Moreover, it is true that the interference modulations may be also found in the Bethe-Heitler cross section generated by the electron scattering in multi-center potentials in the absence of a laser field.

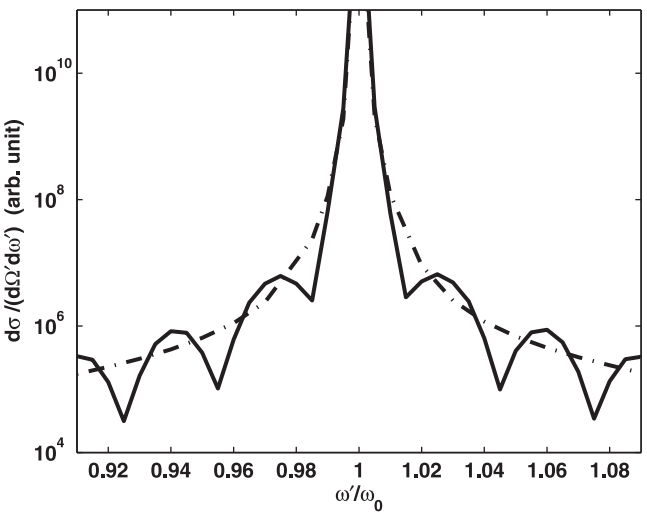

FIG. 6. The cross section for the fundamental harmonic at $\theta' = 1^\circ$. The parameter of the electron and laser is the same with Fig. 3. The internucleus distance is 1 nm and the orientation is $(\vartheta = 0)$ for the full line and $(\vartheta = \pi/2)$ for the dashed line.

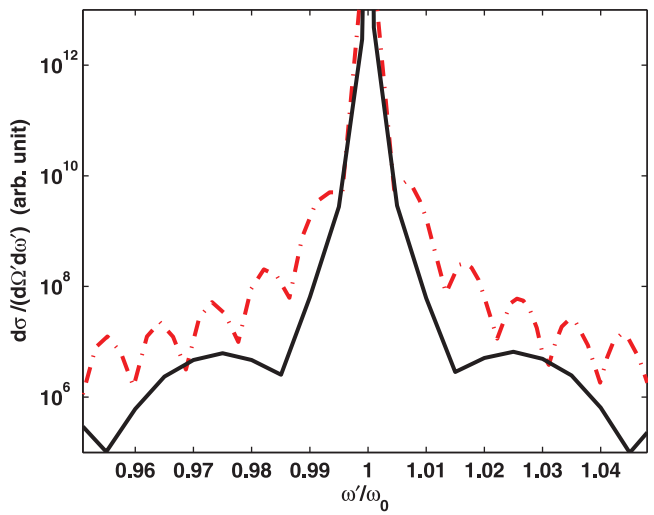

FIG. 7. The cross section for the fundamental harmonic at $\theta' = 1^\circ$. The parameter of the electron and laser is the same with Fig. 3 except that the initial energy of the electron reduces to 3.5 MeV for the dotted-dashed line and 5 MeV for the full line. The internucleus distance is 1 nm.

Considering the appearance of the resonances, we may expect a great difference between the interference modulations of the laser-free spectrum from those of the laser-assisted spectrum we found in this paper (i.e., there will not be minima located symmetrically on each side of the resonance in the laser-free spectrum). Further discussion of the detail about the differences between the two spectrums is beyond the topic of this paper. Furthermore, it is possible to modulate the intensity and the interference diagram of the electron radiation spectrum by controlling the laser field in an actual experiment, for which we think the laser field is helpful in observing a clear interference effect in the spectrum.

IV. CONCLUSION

In this paper, we have investigated the scattering of an electron by the screened Coulomb field of two fixed nuclei in a highly intense laser field and then emit a bremsstrahlung photon. As a result, we found that the spectrum may exhibit minima away from the resonant frequency. This may be explained by the interference between contributions from two fixed nuclei. It was shown that the positions of the interference minima are characteristic of both the internuclear distance and orientation for given laser and electron. On the other hand, the laser intensity and wavelength and the initial electron energy are also responsible for the observed minima. It is shown that the interference effect is remarkable for slow electrons counter-propagating with the laser field. That is due to the large momentum transfer from the Coulomb field. This interference effect is very general in highly intense laser field in which the drift motion of the electron cannot be neglected. Choosing proper laser wavelength, one can obtain information about the molecule structure by detecting the corresponding photon spectrum.

Finally, we must point out that the idea discussed in this paper about the two-center potential can be generalized to more complex potentials to find its important practical applications. For example, the existence of multiply charged negative ions in intense high-frequency laser fields has been studied theoretically for a long time.[20] Recently, by including relativistic corrections, the ions have been found to be able to bind more electrons.[21] How to detect these exotic ions existing only in intense laser fields has posed a great challenge to present experimentalists. Our next work will focus upon analyzing the characteristics of the radiation spectrum when the free electrons are injected upon the negative ions inside the laser fields, for these ions have a very special dressed potential structure just like a many-atom molecule.

ACKNOWLEDGMENTS

This work was supported by the National Natural Science Foundation of China under Grant Nos. 10974056 and 11274117. One of the authors, Wenjun Zhu, thanks the support by the Science and Technology Foundation of National Key Laboratory of Shock Wave and Detonation Physics (Grant No. 077110).

APPENDIX A: DERIVATION OF EQ. (11)

Considering expressions (2), (3), (4), and (9), the transition amplitude of an electron scattering (8) reads as

$$S_{fi} = -\frac{e^2 c}{\hbar^2 c^2}\sqrt{\frac{m^2c^2}{\Pi_i^0 \Pi_f^0 V}}\sqrt{2\pi\hbar/\omega'}T_{fi}.$$

Here,

$$\begin{aligned} T_{fi} &= T_{fi}^{(1)} + T_{fi}^{(2)}, \\ T_{fi}^{(1)} &= \int dx^4 dy^4 \overline{u_{r_f}(p_f)}[\bar{\zeta}_{p_f}(x)\not{\epsilon}_c \zeta_p(x)] iS(x-y) \\ &\quad \times [\bar{\zeta}_p(y)\not{A}_Y(y)\zeta_{p_i}(y)]u_{r_i}(p_i)e^{ik'x}, \\ iS(x-y) &= -\frac{1}{2\pi i}\int \frac{d^4p}{(2\pi\hbar)^3}\frac{1}{\not{p}-mc}. \end{aligned} \tag{A1}$$

$T_{fi}^{(2)}$ can be obtained from T_{fi}^1 by interchanging: $x \to y$, $\not{\epsilon}_c \to \not{A}_Y$.

With the definition of $\zeta_p(x)$ in Eq. (3), it follows the relation

$$\begin{aligned} \bar{\zeta}_{p_f}(x)\not{\epsilon}_c\zeta_p(x) &= \sum_{s_1} M_{s_1}(\not{\epsilon}_c, \eta^1_{\Pi,\Pi_f}, \eta^2_{\Pi,\Pi_f}) \\ &\quad \times e^{i(\Pi_f - \Pi + s_1\hbar k)x/\hbar}, \\ \bar{\zeta}_p(y)\not{A}_Y(y)\zeta_{p_i}(y) &= \sum_{s_2} \overline{M_{s_2}}(\not{A}_Y(y), \eta^1_{\Pi,\Pi_i}, \eta^2_{\Pi,\Pi_i}) \\ &\quad \times e^{i(\Pi_i - \Pi + s_2\hbar k)y/\hbar}. \end{aligned} \tag{A2}$$

During the calculation, the following expression will be useful

$$\begin{aligned} \exp(i\alpha\sin(kx-\varphi) - i\beta\sin 2kx) &= \sum_s G_s^0(\alpha,\beta,\varphi)e^{iskx}, \\ \cos(kx)\exp(i\alpha\sin(kx-\varphi) - i\beta\sin 2kx) &= \sum_s G_s^1(\alpha,\beta,\varphi)e^{iskx}, \\ \sin(kx)\exp(i\alpha\sin(kx-\varphi) - i\beta\sin 2kx) &= \sum_s G_s^2(\alpha,\beta,\varphi)e^{iskx}, \\ \sin(2kx)\exp(i\alpha\sin(kx-\varphi) - i\beta\sin 2kx) &= \sum_s G_s^3(\alpha,\beta,\varphi)e^{iskx}. \end{aligned} \tag{A3}$$

All integrations can be taken in the expression of $T_{fi}^{(1)}$, leaving the energy-conserving delta function: $\delta(\Pi_f - \Pi + s_1\hbar k + \hbar k')$ and $\delta(\Pi_i - \Pi + s_2\hbar k + \hbar q)$, which leads to the energy-momentum conserving relation (14). Finally, the expression for $T_{fi}^{(1)}$ reads

$$\begin{aligned} T_{fi}^{(1)} &= (\hbar^2)\sum_{s,n} A_Y^0(q)\overline{u_{r_f}(p_f)}M_{-n-s}(\not{\epsilon}_c, \eta^1_{\Pi,\Pi_f}, \eta^2_{\Pi,\Pi_f}) \\ &\quad \times \frac{i}{\not{p}-mc} \times \overline{M_{-s}}(\gamma^0, \eta^1_{\Pi,\Pi_i}, \eta^2_{\Pi,\Pi_i})u_{r_i}(p_i) \\ &\quad \times \delta(\Pi_f^0 - \Pi^0 - n\hbar k^0 - \hbar k'^0). \end{aligned} \tag{A4}$$

The expression of $T_{fi}^{(2)}$ is similar to that of $T_{fi}^{(2)}$ by substitutions as follows:

$$\Pi \rightarrow \Pi', \not{\epsilon}_c \rightarrow \gamma^0.$$

Taking the square of the transition amplitude S_{fi}, we will finally have expression (11).

[1]A. McPherson *et al*., J. Opt. Soc. Am. B **4**, 595 (1987).
[2]A. L'Huillier, K. J. Schafer, and K. C. Kulander, J. Phys. B **24**, 3315 (1991).
[3]P. B. Corkum, Phys. Rev. Lett. **71**, 1994 (1993).
[4]M. Lewenstein, Ph. Balcou, M. Yu. Ivanov, A. L'Huillier, and P. B. Corkum, Phys. Rev. A **49**, 2117 (1994).
[5]M. Lein, N. Hay, R. Velotta, J. P. Marangos, and P. L. Knight, Phys. Rev. Lett. **88**, 183903 (2002).
[6]M. Lein, N. Hay, R. Velotta, J. P. Marangos, and P. L. Knight, Phys. Rev. A **66**, 023805 (2002).
[7]R. Kopold, W. Becker, and M. Kleber, Phys. Rev. A **58**, 4022 (1998).
[8]G. Lagmago Kamta and A. D. Bandrauk, Phys. Rev. A **70**, 011404 (R) (2004); **71**, 053407 (2005).
[9]T. Kanai, N. Minemoto, and H. Sakai, Nature (London) **435**, 470 (2005).
[10]C. Vozzi *et al*., Phys. Rev. Lett. **95**, 153902 (2005).
[11]J. Itatani *et al*., Nature (London) **432**, 867 (2004).
[12]G. N. Gibson and J. Biegert, Phys. Rev. A **78**, 033423 (2008).
[13]P. V. Karapetyan and M. V. Fedorov, Zh. Eksp. Teor. Fiz. **75**, 816 (1978).
[14]S. P. Roshchupkin, Laser Phys. **6**, 837 (1996).
[15]S. P. Roshchupkin, Laser Phys. **12**, 498 (2002).
[16]E. Lotstedt, U. D. Jentschura, and C. H. Keitel, Phys. Rev. Lett. **98**, 043002 (2007).
[17]S. Schnez, E. Lotstedt, U. D. Jentschura, and C. H. Keitel, Phys. Rev. A **75**, 053412 (2007).
[18]H. Mitter, Acta Phys. Austriaca, Suppl. **14**, 397 (1975).
[19]A. Ringwald, Phys. Lett. B **510**, 107 (2001).
[20]T. Andersen, Phys. Rep. **394**, 157 (2004).
[21]R. D. Hoehn, J. X. Wang, and S. Kais, J. Chem. Phys. **136**, 034114 (2012).